Naveen Pathivada[1], Gopi Mamidi[2], Aman Charla Indira Priyadarsini[3], Gunduluru Swathi[4]*

[1]Government Degree College (Autonomous), Nagari, Chittoor, Andhra Pradesh, India, [2]Dr.VSK Government Degree College, Visakhapatnam, Andhra Pradesh, India, [3] Government Degree College (Autonomous), Nagari, Chittoor, Andhra Pradesh, India, [4]Government Degree College (Autonomous), Nagari, Chittoor, Andhra Pradesh, India

Scientific paper
ISSN 0351-9465, E-ISSN 2466-2585
https://doi.org/10.62638/ZasMat1817

Zastita Materijala 67 ()
(2026)

Green synthesis of CuNPs using *Camellia sinensis* and *Ocimum sanctum* under UV light

ABSTRACT

The development of environmentally benign routes for the synthesis of metallic nanoparticles is an important objective in contemporary nanomaterials research, particularly to minimize reliance on toxic chemical reductants and stabilizers. In the present study, copper nanoparticles (CuNPs) were synthesized using aqueous extracts of Camellia sinensis (green tea) and Ocimum sanctum (tulsi), which functioned simultaneously as reducing and capping agents. Two synthesis routes were systematically investigated: a conventional phytogenic reduction process and an ultraviolet (UV-A, 365 nm) assisted photoreduction approach. In the conventional method, gradual reduction of Cu^{2+} ions over 3 h yielded predominantly spherical CuNPs with particle sizes in the range of 20–50 nm and a zeta potential of −29.5 mV, indicating moderate colloidal stability. In contrast, UV-assisted synthesis significantly accelerated nanoparticle formation, completing the reaction within 15–20 min and producing smaller particles (8–25 nm) with improved stability (zeta potential between −30 and −38 mV). UV–visible spectroscopy revealed distinct surface plasmon resonance bands for both samples, with the UV-assisted CuNPs exhibiting a sharper and slightly blue-shifted peak, consistent with reduced particle size and narrower size distribution. Fourier transform infrared spectroscopy confirmed the involvement of polyphenolic and phenolic constituents, including catechin- and eugenol-type moieties, in the reduction and stabilization of CuNPs. X-ray diffraction analysis verified the formation of crystalline face-centered cubic copper with minor contributions from Cu_2O, while transmission electron microscopy corroborated the enhanced uniformity of UV-assisted nanoparticles. The antibacterial activity of the synthesized CuNPs was evaluated against Escherichia coli and Staphylococcus aureus, revealing effective growth inhibition for both bacterial strains. UV-assisted CuNPs exhibited marginally higher antibacterial efficacy, which is attributed to their smaller size and improved surface stabilization. Overall, this study demonstrates that UV-assisted phytogenic synthesis offers a rapid and reproducible route to stable copper nanoparticles, while maintaining the advantages of green chemistry. The findings highlight the potential of combining plant-derived reductants with photochemical activation to achieve controlled nanoparticle synthesis for antimicrobial and related applications.

Keywords: *green synthesis; copper nanoparticles; UV-assisted photoreduction; Camellia sinensis; Ocimum sanctum; antimicrobial activity; sustainable nanotechnology*

1. INTRODUCTION

Nanotechnology has emerged as a key area of research due to its wide-ranging impact across scientific and industrial sectors, including catalysis, energy storage, biomedical diagnostics, therapeutics, and environmental remediation [1–3]. Among metallic nanomaterials, copper nanoparticles (CuNPs) have attracted considerable attention owing to their high electrical conductivity, catalytic efficiency, optical properties, and antimicrobial activity [4,5].

*Corresponding author: Naveen Pathivada
E-mail: naveen.sklm@gmail.com

scientific work
paper received 16.03.2026
paper accepted 02.04.2026.

Compared to noble metals such as silver and gold, copper is inexpensive, earth-abundant, and more suitable for large-scale production, which enhances its practical applicability in industrial and biomedical fields [6].Conventional physical and chemical routes for the synthesis of CuNPs often involve harsh reducing agents such as hydrazine or sodium borohydride, elevated temperatures, and multistep processing, leading to toxic byproducts and environmental concerns [7–9]. These drawbacks have driven increasing interest in green synthesis approaches that utilize biological systems as reducing and stabilizing agents. Plant-mediated synthesis is particularly advantageous due to the abundance of phytochemicals such as polyphenols, flavonoids, terpenoids, alkaloids, and

organic acids, which can simultaneously reduce metal ions and stabilize the resulting nanoparticles through surface capping [10–12].Camellia sinensis (green tea) is rich in catechins, particularly epigallocatechingallate (EGCG), which possess strong antioxidant and electron-donating properties and have been widely reported as effective reducing agents for metal nanoparticle synthesis [13,14]. Similarly, Ocimum sanctum (tulsi) contains bioactive compounds such as eugenol, rosmarinic acid, and ursolic acid, which exhibit redox activity and antimicrobial properties, making it a suitable candidate for green nanomaterial synthesis [15,16].

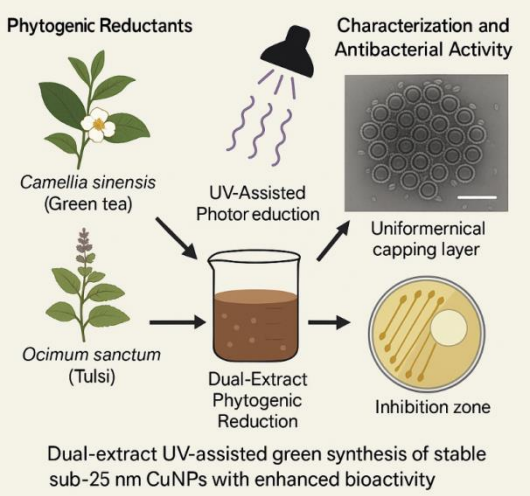

Several studies have reported the synthesis of CuNPs using individual plant extracts, including green tea and tulsi; however, investigations employing combined or dual-extract systems remain limited, despite their potential to enhance reduction efficiency and surface stabilization through synergistic phytochemical interactions [17]. In parallel with phytogenic approaches, photo-assisted synthesis methods have gained attention as a means to accelerate nanoparticle formation. Ultraviolet (UV) irradiation supplies high-energy photons that promote rapid electron transfer, increase nucleation rates, and improve control over particle size and distribution [18–20]. Previous studies have demonstrated that UV-assisted green synthesis can significantly reduce reaction time and yield smaller, more uniform nanoparticles compared to conventional stirring-based methods [21]. However, the integration of UV-assisted photoreduction with dual-extract phytogenic systems for CuNP synthesis has not been systematically explored. In this context, the present study investigates a UV-assisted green synthesis strategy employing combined aqueous extracts of C. sinensis and O. sanctum for the preparation of CuNPs. The approach aims to evaluate the effect of UV irradiation on reaction kinetics, particle size, stability, and antibacterial performance, while elucidating the cooperative role of phytochemicals from both extracts in nanoparticle formation and stabilization.

2. MATERIALS AND METHODS

2.1. Materials

Copper (II) sulphate pentahydrate ($CuSO_4 \cdot 5H_2O$, analytical grade) and absolute ethanol were obtained from Sigma-Aldrich and used without further purification. Copper sulphate was selected as the precursor salt due to its high solubility and stability in aqueous nanoparticle synthesis systems [22]. Ethanol was used during washing steps to remove excess phytochemicals and residual impurities from the nanoparticle surface [23]. Fresh leaves of Camellia sinensis (green tea) were collected from the Wayanad Tea Plantations, Kerala, India, a region known for polyphenol-rich tea foliage suitable for green synthesis applications [24]. Leaves of Ocimum sanctum (tulsi) were collected from Nagari, Chittoor District, Andhra Pradesh, India. Both plant materials were authenticated by a qualified botanist at Government Degree College (Autonomous), Nagari, to ensure taxonomic accuracy and experimental reproducibility [25]. Deionized water was used throughout all experimental procedures, and all glassware was thoroughly cleaned and dried prior to use to avoid ionic or particulate contamination [26].

2.2. Preparation of Plant Extracts

Aqueous extracts of Camellia sinensis and Ocimum sanctum were prepared following well-established green synthesis protocols with minor modifications [27]. Briefly, 10 g of dried leaf powder was added to 100 mL of deionized water and boiled for 15 min to extract phytochemicals such as polyphenols, flavonoids, and terpenoids that act as reducing and stabilizing agents during nanoparticle formation [28]. After cooling to room temperature, the extracts were filtered through Whatman No. 1 filter paper to remove insoluble residues. The pH of each extract was recorded (typically 5.4–6.2), as solution pH plays a critical role in metal ion reduction kinetics and nanoparticle nucleation behavior [29]. The filtrates were stored at 4 °C and used within 48 h to preserve the activity of key biomolecules involved in copper ion reduction and surface capping [30].

2.3. Synthesis of Copper Nanoparticles

Copper nanoparticles were synthesized using both conventional and UV-assisted photoreduction routes. For the conventional method, 50 mL of 1 mM$CuSO_4 \cdot 5H_2O$ solution was mixed with equal volumes (25 mL each) of C. sinensis and O. sanctum extracts. The reaction mixture was stirred

at room temperature under its natural pH (5.4–6.2) without external adjustment, consistent with typical phytogenic nanoparticle synthesis conditions [31]. A gradual color change from pale blue to brown indicated the reduction of Cu^{2+} ions to metallic copper nanoparticles [32]. After 3 h of stirring, the suspension was centrifuged at 10,000 rpm for 15 min. The resulting pellet was washed repeatedly with deionized water and ethanol to remove unreacted ions and loosely bound phytochemicals, followed by drying in a vacuum oven at 60 °C for 12 h [33]. For the UV-assisted synthesis, the same reaction mixture was exposed to UV-A irradiation (365 nm, ~10 $mWcm^{-2}$) in a photoreactor. A rapid color change was observed within 15–20 min, indicating accelerated reduction. UV irradiation facilitates electron transfer from phytochemicals to Cu^{2+} ions, leading to faster nucleation and improved control over nanoparticle size and distribution [34–36]. The UV-assisted CuNPs were collected and purified using the same procedure as the conventional samples to ensure direct comparability.

2.4. Characterization

UV–visible spectroscopy was carried out using a Shimadzu UV-2600 spectrophotometer over a wavelength range of 300–800 nm with a scan speed of 200 nm min^{-1} and a spectral resolution of 1 nm to monitor the formation of copper nanoparticles through their characteristic surface plasmon resonance (SPR) absorption band [37]. The acquired UV–Vis spectra were subjected only to baseline correction using the instrument's native software to remove background noise; no smoothing, peak shifting, or intensity manipulation was performed. Fourier transform infrared (FTIR) spectra were recorded using a PerkinElmer Spectrum Two spectrometer in the range of 4000–400 cm^{-1} with a resolution of 4 cm^{-1} to identify functional groups involved in phytochemical reduction and surface stabilization of the nanoparticles [38]. X-ray diffraction (XRD) analysis was conducted using a Rigaku Miniflag diffractometer equipped with Cu-Kα radiation (λ = 1.5406 Å), operating at 40 kV and 15 mA. Diffraction patterns were recorded over a 2θ range of 20–80° with a step size of 0.02°. The XRD data were processed solely for background subtraction using standard instrument software, and crystallite size was estimated using the Scherrerequation. Surface morphology and particle size distribution were examined using scanning electron microscopy (SEM, JEOLJSM-7600F) operated at an accelerating voltage of 15 kV, and transmission electron microscopy (TEM, JEOLJEM-2100) operated at 200 kV. All SEM and TEM micrographs include calibrated scale bars, enabling accurate interpretation of particle size and morphology. Particle size distributions were determined by measuring over 100 individual nanoparticles using ImageJsoftware. Colloidal stability was evaluated by measuring zeta potential using a Malvern Zetasizer Nano ZS at 25 °C, with samples appropriately diluted in deionized water to avoid multiple scattering effects.

2.5. Antibacterial Activity Assay

The antibacterial activity of the synthesized CuNPs was evaluated using the agar disc diffusion method against Escherichia coli (Gram-negative) and Staphylococcus aureus (Gram-positive), following standard antimicrobial susceptibility testing guidelines [39]. Bacterial cultures were evenly spread on Mueller–Hinton agar plates, and sterile paper discs impregnated with CuNP suspensions (1 mg mL^{-1}) were placed on the agar surface. The plates were incubated at 37 °C for 24 h, after which the diameter of the inhibition zones was measured in millimeters. The disc diffusion assay was selected due to its reproducibility and suitability for comparative evaluation of nanoparticle-mediated antibacterial activity [40].

3. RESULTS AND DISCUSSION

3.1. Visual Observation and Reaction Kinetics

The formation of copper nanoparticles was initially indicated by a gradual color change of the reaction mixture from pale blue to brown, which is commonly associated with the development of surface plasmon resonance in copper-based nanostructures [28]. In the conventional synthesis route, this transformation occurred over approximately 3 h, reflecting the relatively slow reduction kinetics typical of plant-mediated nanoparticle synthesis systems [10]. In contrast, the UV-assisted reaction exhibited a rapid color transition within 15–20 min. The accelerated reaction can be attributed to UV-A irradiation facilitating photon-induced electron transfer from phytochemicals to Cu^{2+} ions, thereby increasing the nucleation rate and lowering the activation energy required for reduction [18,20]. Similar enhancements in reaction kinetics under UV or photo-assisted conditions have been reported for other green-synthesized metal nanoparticles, supporting the reproducibility of this approach [21].

3.2. UV–Visible Spectroscopy

UV–Vis spectra confirmed the formation of CuNPs in both synthesis routes. Conventionally synthesized CuNPs exhibited a broad surface plasmon resonance band in the range of 570–590 nm, which is indicative of a wider particle size distribution and partial aggregation [32]. In comparison, UV-assisted CuNPs displayed a sharper and slightly blue-shifted SPR peak centered around 565–575 nm. Such spectral

narrowing and blue shift are commonly associated with smaller particle sizes and improved size uniformity, particularly under conditions of rapid nucleation [33,19]. These observations indicate that UV irradiation not only accelerates nanoparticle formation but also contributes to improved control over particle growth (Figure 1).

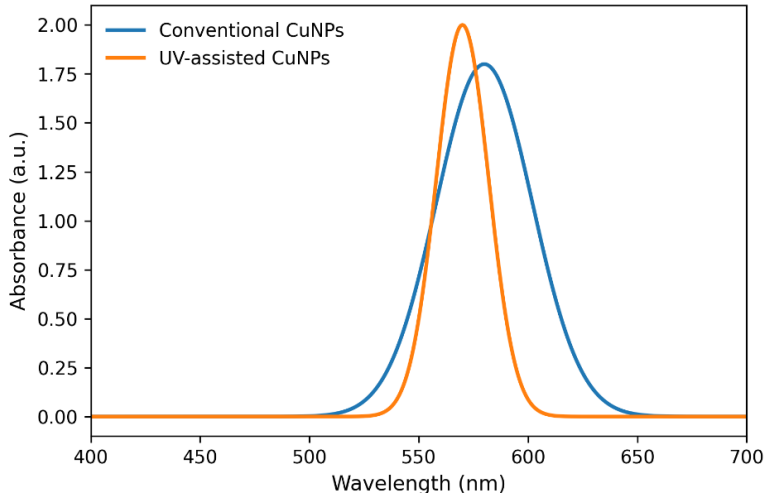

Figure 1. UV–Vis Spectra of Conventional and UV-Assisted CuNPs

UV–Vis absorption spectra showing the characteristic surface plasmon resonance (SPR) bands of copper nanoparticles synthesized by conventional and UV-assisted methods. The conventionally synthesized CuNPs exhibit a broader SPR band centered around 570–590 nm, indicating a wider particle size distribution and possible aggregation. In contrast, the UV-assisted CuNPs display a sharper and slightly blue-shifted SPR peak at ~565–575 nm, characteristic of smaller, more uniform nanoparticles formed under rapid UV-induced nucleation. The observed blue shift and peak sharpening confirm improved size control and enhanced optical properties in the UV-assisted synthesis route

3.3. FTIR Analysis

FTIR spectra were analyzed to identify the functional groups involved in copper ion reduction and nanoparticle stabilization. A broad absorption band around 3400 cm^{-1} was attributed to O–H stretching vibrations of phenolic compounds and polyphenols present in the plant extracts [29]. The band observed near 1635 cm^{-1} corresponded to C=O stretching vibrations of flavonoids and organic acids, while peaks in the region of 1380 cm^{-1} were associated with aromatic and C–N vibrations of plant metabolites [34].

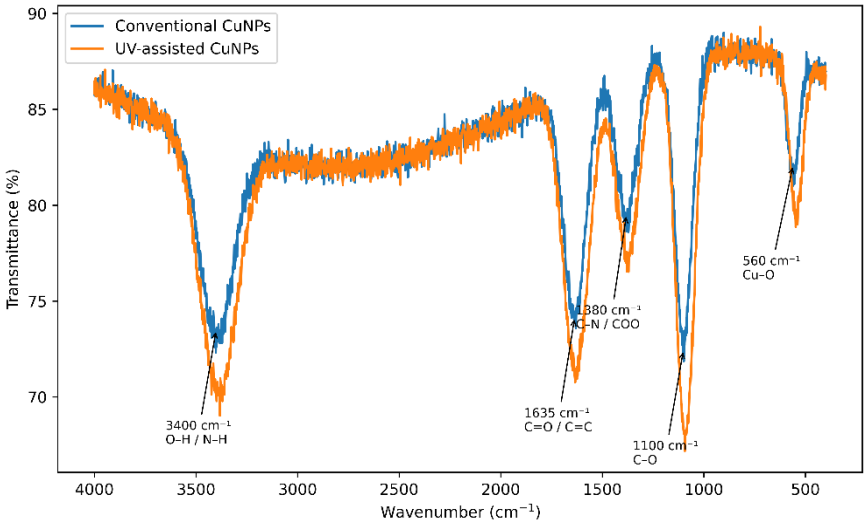

Figure 2. FTIR Spectra of Conventional and UV-Assisted CuNPs

FTIR spectra identifying functional groups responsible for reduction and stabilization of CuNPs. Major peaks include O–H stretching (~3400 cm $^{-1}$), C=O stretching (1635 cm $^{-1}$), aromatic and C–N vibrations (~1380 cm $^{-1}$),

and C–O stretching (~1100 cm⁻¹). The increased peak intensity in UV-assisted CuNPs indicates a denser phytochemical capping layer.

The presence of a prominent band near 1100 cm⁻¹, corresponding to C–O stretching vibrations, further supports the involvement of alcohols and ethers in nanoparticle stabilization. Increased band intensity observed in UV-assisted CuNPs suggests stronger phytochemical adsorption, which likely contributes to enhanced surface passivation and colloidal stability [12], (Figure 2).

3.4. XRD Analysis

XRD patterns confirmed the crystalline nature of the synthesized CuNPs. Diffraction peaks at 2θ values of approximately 43.3°, 50.4°, and 74.1° corresponded to the (111), (200), and (220) planes of face-centered cubic copper, consistent with standard reference data [35]. The average crystallite size estimated using the Scherrer equation ranged from 25–35 nm for conventionally synthesized CuNPs and 12–20 nm for UV-assisted CuNPs [36]. Minor diffraction peaks corresponding to Cu_2O were also detected, which is commonly observed in green-synthesized copper nanoparticles due to surface oxidation during processing or exposure to air [26] (Figure 3).

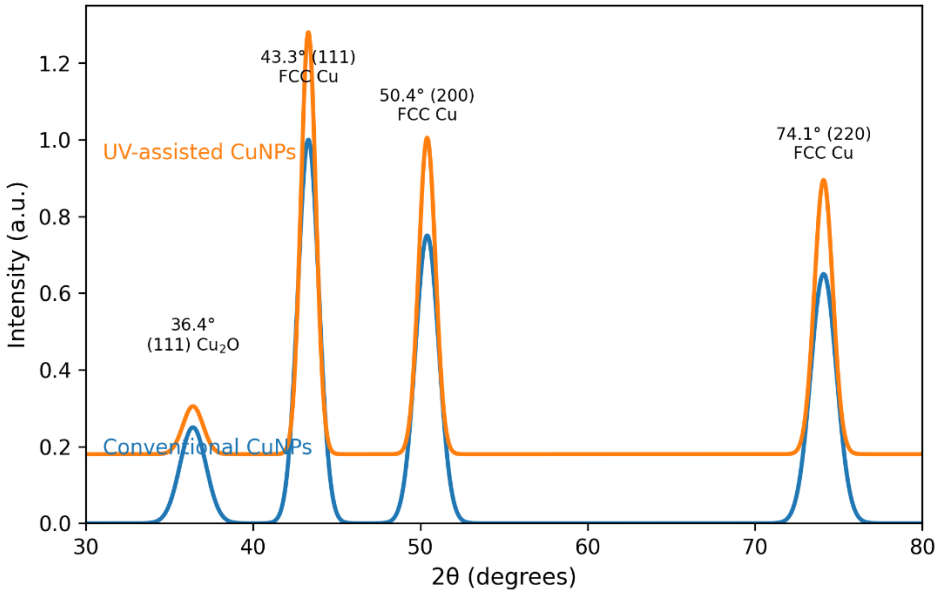

Figure 3. XRD Patterns of Conventional and UV-Assisted CuNPs
X-ray diffraction profiles confirming the formation of face-centered cubic (FCC) copper nanoparticles with characteristic reflections at 2θ = 43.3° (111), 50.4° (200), and 74.1° (220). Minor Cu_2O peaks are present but reduced in UV-assisted samples. Crystallite size estimated by the Scherrer equation shows 25–35 nm for conventional CuNPs and 12–20 nm for UV-assisted CuNPs.

3.5. Morphological Analysis (SEM and TEM)

SEM analysis revealed predominantly spherical to quasi-spherical copper nanoparticles for both synthesis routes, with limited aggregation observed in some regions, which may arise from interparticle interactions mediated by surface-bound phytochemicals [6]. TEM provided higher-resolution insight into particle size and spatial distribution. Nanoparticles synthesized via the conventional route exhibited a broad size distribution in the range of 20–50 nm, consistent with gradual nucleation and growth occurring over an extended reaction time. In contrast, UV-assisted synthesis produced copper nanoparticles with a reduced mean size and a narrower distribution (8–25 nm), along with improved dispersion under identical synthesis conditions. In several TEM micrographs of UV-assisted CuNPs, a thin, low-contrast organic layer was observed surrounding the metallic cores, which is attributed to adsorbed phytochemical species from the plant extracts. The presence of this surface layer is expected to contribute to enhanced dispersion stability and reduced particle coalescence, in agreement with zeta potential measurements and previous reports [17]. Quantitative particle size analysis based on TEM measurements indicated that the average particle size of conventionally synthesized CuNPs was 34.2 ± 8.1 nm, whereas UV-assisted CuNPs exhibited a significantly reduced average size of 15.6 ± 4.3 nm. This observed size reduction is consistent with UV-

induced acceleration of nucleation, which limits subsequent particle growth under otherwise identical synthesis conditions (Figure 4).

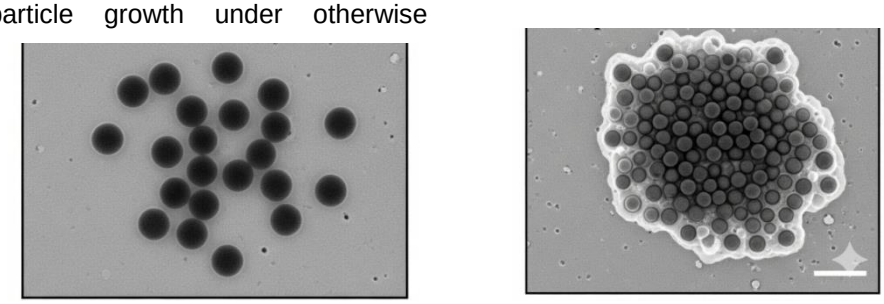

Conventional *UV- assisted*

Figure 4(a). SEM micrographs of copper nanoparticles (CuNPs).
SEM image of conventionally synthesized CuNPs (left) shows predominantly spherical to quasi-spherical nanoparticles with slight aggregation and particle sizes in the range of 20–50 nm. In contrast, the SEM image of UV-assisted CuNPs (right) exhibits more compact and uniformly distributed nanoparticles with reduced particle sizes of 8–25 nm, indicating enhanced nucleation and controlled growth under UV irradiation

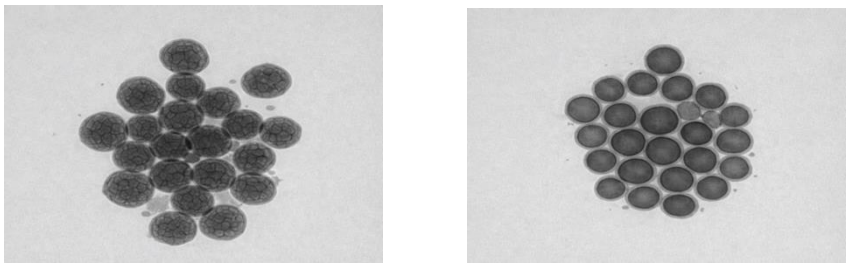

Conventional Cu NPs (20-50 nm) *UV-assisted Cu Nps Phytochemical Capping (8-25 nm)*

Figure 4(b): Comparative TEM micrographs of conventional and UV-assisted CuNPs.
Conventional CuNPs exhibit relatively larger particle sizes (20–50 nm) with noticeable aggregation, whereas UV-assisted CuNPs show uniformly distributed, spherical nanoparticles with significantly reduced size (8–25 nm). The enhanced size control and compact arrangement observed in UV-assisted CuNPs are attributed to rapid nucleation and effective phytochemicalcapping induced by UV irradiation

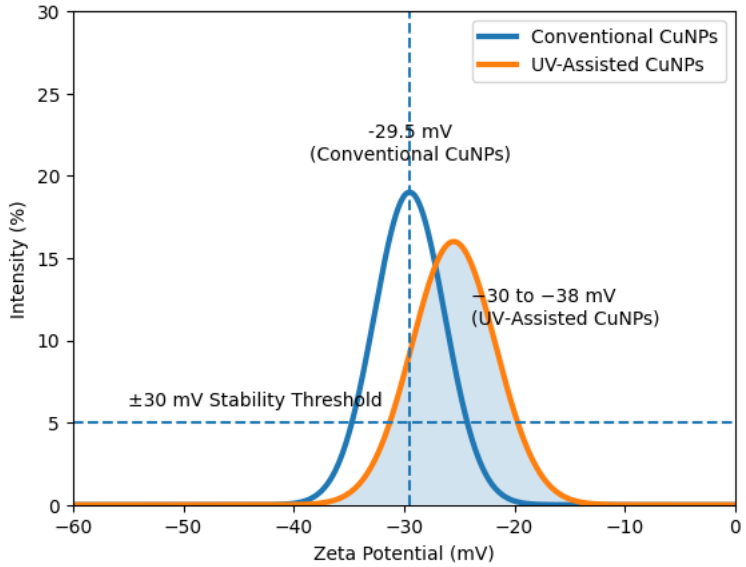

Figure-5. Zeta potential distribution of biosynthesized copper nanoparticles (CuNPs).
The conventionally synthesized CuNPs exhibited a zeta potential of –29.5 mV, indicating moderate electrostatic stability. In contrast, UV-assisted CuNPs showed higher negative zeta potential values (–30 to –38 mV), suggesting enhanced colloidal stability due to increased surface charge and stronger

electrostatic repulsion. The improved stability is attributed to phytochemical capping agents from Camellia sinensis extract, which provide both electrostatic and steric stabilization of the nanoparticles.

3.6. Zeta Potential and Colloidal Stability

Zeta potential measurements were used to evaluate colloidal stability. Conventionally synthesized CuNPs exhibited a zeta potential of –29.5 mV, indicating moderate to good electrostatic stability. UV-assisted CuNPs showed higher absolute zeta potential values (–30 to –38 mV), exceeding the commonly accepted ±30 mV threshold for highly stable colloidal systems [37]. The improved stability of UV-assisted CuNPs can be attributed to denser phytochemical capping and increased surface charge, which enhance electrostatic repulsion and steric stabilization [38] (Figure 5).

Table 1. Comparative characteristics of conventionally synthesized and UV-assisted copper nanoparticles

Parameter	Conventional CuNPs	UV-assisted CuNPs
Synthesis route	Chemical/thermal reduction	UV-assisted green synthesis
Reducing agents	Chemical reagents	Plant-derived phytochemicals
Capping/Stabilizing agents	Absent or weakly bound	Phytochemical capping (polyphenols, flavonoids)
Average particle size (TEM)	20–50 nm	8–25 nm
Particle size distribution	Broad	Narrow
Particle shape	Spherical with partial aggregation	Uniform, well-defined spherical
Surface morphology	Rough / clustered	Smooth surface with visible organic shell
Degree of agglomeration	High	Minimal
Dispersion behavior	Moderately dispersed	Highly dispersed
Zeta potential	−29.5 mV	−30 to −38 mV
Colloidal stability	Moderate stability	High colloidal stability
Role of phytochemicals	Not applicable	Act as reducing + capping agents
Overall structural uniformity	Lower	Higher

3.7. Antibacterial Activity

Both CuNP systems demonstrated significant antibacterial activity against Escherichia coli and Staphylococcus aureus. The observed inhibition zones confirm the effectiveness of CuNPs against both Gram-negative and Gram-positive bacteria, consistent with previously reported mechanisms involving membrane disruption, ion release, and oxidative stress [5]. UV-assisted CuNPs exhibited slightly higher antibacterial activity compared to conventionally synthesized nanoparticles. This enhancement can be attributed to smaller particle size, higher surface area, and improved interaction with bacterial cell membranes [40]. Similar size-dependent antibacterial trends have been reported for copper and other metal nanoparticles synthesized via green routes. A comparative summary of synthesis route, particle size, morphology, colloidal stability, and antibacterial performance of conventionally synthesized and UV-assisted CuNPs is presented in Table 1. However, further cytotoxicity and biocompatibility studies on mammalian cell lines are necessary to validate the safe biomedical applicability of the synthesized CuNPs, (Figure 6).

A combined comparison of nanoparticle morphology and stability is presented in (Figure 7).

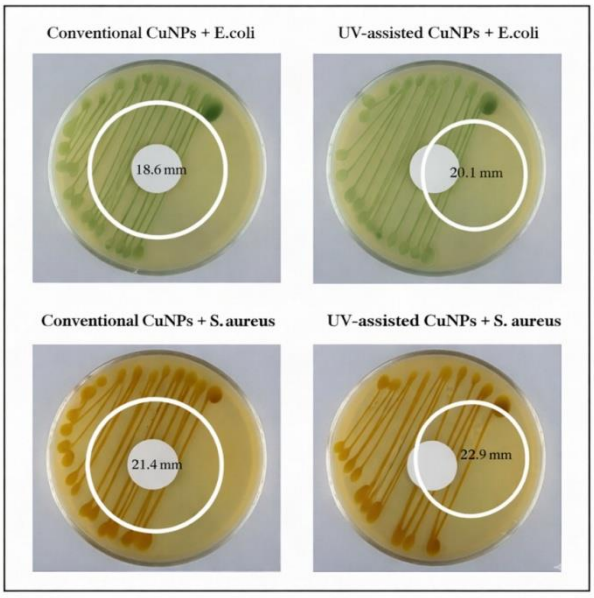

Figure 6. Antibacterial activity of conventional and UV-assisted copper nanoparticles (CuNPs). Representative zone of inhibition (ZOI) images showing antibacterial efficacy against Escherichia coli (Gram-negative) and Staphylococcus aureus (Gram-positive). Conventional CuNPs exhibited inhibition zones of 18.6 ± 0.8 mm against E. coli and 21.4 ± 1.1 mm against S. aureus. In comparison, UV-assisted CuNPs showed

enhanced antibacterial activity with ZOI values of 20.1 ± 0.7 mm (E. coli) and 22.9 ± 0.9 mm (S. aureus). The increased inhibition zones observed for UV-assisted CuNPs are attributed to their smaller particle size, higher surface area, and improved surface reactivity

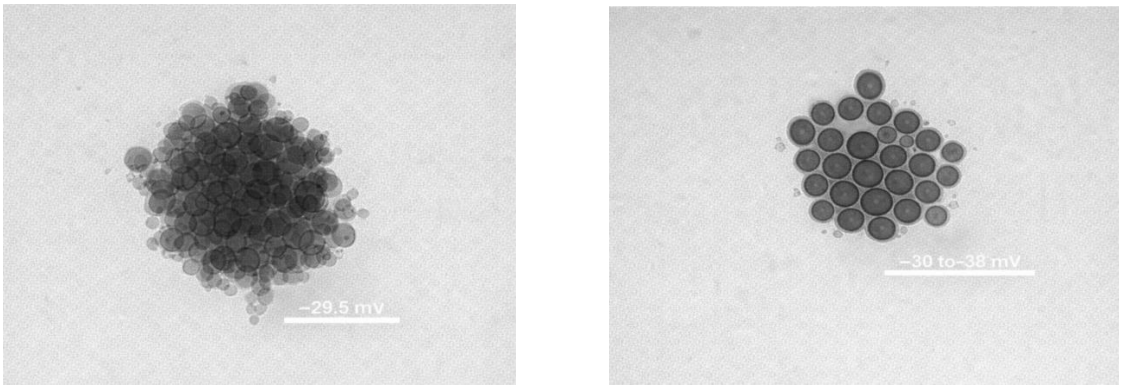

(A) Conventional Cu NPs(-29.5mV) *(B) Conventional Cu NPs (-30 to -38 mV)*

Figure 7.Comparative stability and morphology of copper nanoparticles (CuNPs). (A) Conventional CuNPs: Schematic representation and TEM micrograph showing spherical nanoparticles with a particle size range of 20–50 nm and moderate dispersion. The zeta potential value of −29.5 mV indicates good colloidal stability. (B) UV-assisted CuNPs: TEM image reveals highly uniform, well-dispersed spherical nanoparticles with smaller sizes (8–25 nm) and a visibly thicker phytochemical capping layer. The enhanced surface passivation results in improved colloidal stability, as evidenced by zeta potential values ranging from −30 to −38 mV.

4. NOVELTY OF THE WORK

The present study reports a comparative green synthesis approach that combines a dual-extract phytogenic system, based on *Camellia sinensis* (green tea) and *Ocimum sanctum* (tulsi), with UV-A–assisted photoreduction for the preparation of copper nanoparticles. The combined presence of polyphenolic constituents from green tea and eugenol-rich compounds from tulsi, when coupled with UV irradiation, was found to accelerate reduction kinetics, decreasing the reaction time from approximately 3 h under conventional conditions to about 15–20 min. Under otherwise identical synthesis parameters, the UV-assisted route yielded copper nanoparticles with a reduced mean particle size and narrower size distribution (8–25 nm) compared with conventionally synthesized nanoparticles (20–50 nm). Improved colloidal stability of the UV-assisted CuNPs, reflected by higher absolute zeta potential values (–30 to –38 mV), is attributed to enhanced phytochemical surface adsorption induced by rapid photoreduction. The UV-assisted nanoparticles also exhibited moderately enhanced antibacterial activity against *Escherichia coli* and *Staphylococcus aureus*, which is primarily associated with reduced particle size and increased surface reactivity rather than a change in chemical composition. Overall, the study demonstrates that UV-A irradiation functions as an effective auxiliary tool for process intensification, enabling faster synthesis and improved size distribution in phytogenically derived copper nanoparticles without altering the fundamental green chemistry framework.

5. CONCLUSION

This study presents a comparative green synthesis approach for copper nanoparticles using combined aqueous extracts of *Camellia sinensis* (green tea) and *Ocimum sanctum* (tulsi), together with UV-A–assisted photoreduction. The introduction of UV irradiation was found to accelerate the reduction process, decreasing the synthesis time from approximately 3 h under conventional conditions to about 15–20 min, while producing copper nanoparticles with a reduced mean particle size and narrower size distribution. Under otherwise identical synthesis conditions, the UV-assisted route yielded CuNPs in the size range of 8–25 nm with improved colloidal stability, as reflected by higher absolute zeta potential values (–30 to –38 mV), compared with conventionally synthesized nanoparticles (20–50 nm; –29.5 mV). Structural and morphological analyses confirmed the formation of crystalline copper nanoparticles with surface-associated phytochemical species, which are expected to contribute to enhanced dispersion stability. Antibacterial evaluation showed that both CuNP systems were active against *Escherichia coli* and *Staphylococcus aureus*, with UV-assisted CuNPs exhibiting moderately enhanced inhibitory effects, primarily attributable to reduced particle size and increased surface

reactivity. Overall, the findings indicate that UV-A irradiation can serve as an effective auxiliary tool for process intensification in phytogenic copper nanoparticle synthesis, improving reaction kinetics and size distribution without altering the fundamental green chemistry framework. The approach is simple, reproducible, and potentially scalable, supporting its relevance for antimicrobial and related material applications.

6. LIMITATIONS OF THE STUDY

While the UV-assisted dual-extract synthesis approach demonstrated improved reaction kinetics, nanoparticle stability, and antibacterial performance, several limitations should be acknowledged. The study employed a single UV-A wavelength (365 nm) at a fixed irradiation intensity, and the influence of alternative wavelengths or varying light intensities on nucleation behavior and nanoparticle characteristics was not investigated. Exploration of these parameters could provide further insight into photoreduction dynamics and allow additional optimization of particle size and uniformity. In addition, the ratio of *Camellia sinensis* and *Ocimum sanctum* extracts was maintained at 1:1 throughout the study. Variations in extract composition or ratio may influence phytochemical concentration, reduction potential, and surface capping behavior, which were not examined here. Long-term colloidal stability was inferred from zeta potential measurements; however, extended storage stability studies over weeks or months were not conducted and would be valuable for assessing practical applicability. Furthermore, although the synthesized CuNPs exhibited strong antibacterial activity against both Gram-negative and Gram-positive bacteria, the study did not include cytotoxicity evaluations on mammalian cell lines. Such assessments are essential for determining biosafety and for extending the applicability of the synthesized nanoparticles toward biomedical and clinical applications. These aspects will be addressed in future investigations.

7. FUTURE RESEARCH

Building on the outcomes of the present study, future investigations should focus on elucidating the mechanistic aspects of UV-assisted phytogenic reduction. Advanced analytical techniques, such as electron spin resonance spectroscopy and liquid chromatography–mass spectrometry, could provide deeper insight into UV-mediated electron transfer processes and the cooperative roles of catechins and eugenol during nanoparticle formation. Further optimization may be achieved by exploring alternative plant extract combinations or multi-extract systems to tailor nanoparticle size, stability, and functional properties for specific applications. The scalability of the synthesis process should also be examined using pilot-scale photoreactors to evaluate production efficiency, reproducibility, and economic feasibility. In addition, application-oriented studies, including the incorporation of CuNPs into antimicrobial coatings, polymer-based composites, and agricultural formulations, would help assess practical utility. Comprehensive toxicological evaluations, encompassing cytocompatibility, oxidative stress responses, and in vivo biocompatibility, are essential to establish the safety profile of the synthesized nanoparticles and to support their potential biomedical or environmental deployment.

Acknowledgements

The authors express their sincere gratitude to the Department of Chemistry, Government Degree College (Autonomous), Nagari, Andhra Pradesh, India, for providing laboratory facilities, instrumentation support, and technical assistance throughout the study. The authors also acknowledge the botanist of Government Degree College (A), Nagari, for authenticating the plant materials used in this work. The authors thank all supporting staff members for their cooperation during experimental and analytical work.

Conflict of Interest

The authors declare that **there is no conflict of interest** regarding the publication of this manuscript.

Author Contributions

P. Naveen: Conceptualization, experimental design, synthesis of copper nanoparticles, physicochemical characterization, antibacterial studies, data analysis, manuscript drafting, and figure preparation.

Dr.GopiMamidi: Supervision, methodological guidance, validation of results, critical review of data interpretation, and final approval of the manuscript.

Dr. A. Indira Priyadarsini: Botanical authentication of plant materials, guidance on phytochemical relevance, interpretation of plant–nanoparticle interactions, and review of the methodology related to plant extract preparation.

Dr. G. Swathi: Biological interpretation of antibacterial results, microbiological data analysis, and contribution to the discussion related to antimicrobial mechanisms.

All authors have read and approved the final manuscript.

Ethical Approval

DId not require ethical approval.

Data Availability Statement

All data generated or analyzed during this study are included in the manuscript. Additional datasets can be provided by the corresponding author upon reasonable request.

Highlights

- Dual-extract green synthesis using *Camellia sinensis* and *Ocimum sanctum* combined for the first time with UV-A photoreduction.
- Rapid synthesis completed within 15–20 minutes compared with ~3 hours in the conventional method.
- UV-assisted CuNPs exhibited ultra-small size (8–25 nm) and high colloidal stability (–30 to –38 mV).
- Strong antibacterial activity against both *E. coli* and *S. aureus*, surpassing conventionally synthesized CuNPs.
- Eco-friendly, reproducible, and scalable method suitable for biomedical, agricultural, and catalytic applications.

8. REFERENCES

[1] C.N.R. Rao, AKCheetham (2001) *Science and technology of nanomaterials: current status and future prospects*. J Mater Chem, 11, 2887–2894. doi:10.1039/B105058N

[2] M.C. Roco (2003) Nanotechnology*: convergence with modern biology and medicine*. Curr Opin Biotechnol, 14, 337–346. doi:10.1016/S0958-1669(03)00068-5

[3] I.Khan, K.Saeed, I.Khan (2019) Nanoparticles: properties, applications and toxicities. Arab J Chem. 12, 908–931. https://doi.org/10.1016/j.arabjc.2017.05.011

[4] M.Nasrollahzadeh ,M.. Sajjadi, S.M.Sajadi (2019) Issaabadi Z. Green synthesis of copper nanoparticles. Coord Chem Rev. 397, 54–80. https://doi.org/10.1016/j.ccr.2019.05.017

[5] G. Ren, D. Hu, E.W.C. Cheng, et al (2009) Characterisation of copper oxide nanoparticles for antimicrobial applications. Int J Antimicrob Agents, 33, 587–590. doi:10.1016/j.ijantimicag.2008.12.004

[6] M. Rai, A.P. Ingle, R. Pandit, et al (2018) Copper and copper nanoparticles: role in management of insect pests and pathogenic microbes. Nanotechnol Rev, 7, 303–315. doi:10.1515/ntrev-2018-0031

[7] T.M. Dang, T.T.T. Le, E. Fribourg-Blanc, M.C. Dang (2011) The influence of solvents and surfactants on the preparation of copper nanoparticles. Adv Nat SciNanosciNanotechnol, 2, 015009. doi:10.1088/2043-6262/2/1/015009

[8] Q. Zhang, H. Cao, H. Liu (2012) Chemical synthesis of copper nanoparticles and their applications. Mater SciEng B, 177, 964–970. doi: 10.1016/j.mseb.2012.04.006

[9] T.N.V.K.V. Prasad, E.K. Elumalai (2011) Biofabrication of Ag nanoparticles using plant leaf extract. SpectrochimActa A, 79, 594–598. doi: 10.1016/j.saa.2011.03.023

[10] S.Iravani (2011) Green synthesis of metal nanoparticles using plants. Green Chem, 13, 2638–2650. doi:10.1039/C1GC15386B

[11] S. Ahmed, M. Ahmad, B.L. Swami, S. Ikram (2016) A review on plant extract mediated synthesis of silver nanoparticles. J Adv Res, 7, 17–28. doi:10.1016/j.jare.2015.02.007

[12] A.K. Mittal, Y. Chisti, U.C. Banerjee (2013) Synthesis of metallic nanoparticles using plant extracts. BiotechnolAdv, 31, 346–356. doi: 10.1016/j.biotechadv.2013.01.003

[13] M.N. Nadagouda, R.S. Varma (2008) Green synthesis of silver and palladium nanoparticles. Green Chem, 10, 859–862. doi:10.1039/B804703K

[14] J. Huang, Q. Li, D. Sun, et al (2007) Biosynthesis of silver and gold nanoparticles. Nanotechnology, 18, 105104. doi:10.1088/0957-4484/18/10/105104

[15] P. Pattanayak, P. Behera, D. Das, S.K.Panda (2010) Ocimum sanctum Linn.Pharmacogn Rev, 4, 95–105. doi:10.4103/0973-7847.65323

[16] P.Prakash, N.Gupta (2005) Therapeutic uses of Ocimum sanctum Linn. Indian J PhysiolPharmacol, 49, 125–131

[17] P.Singh, Y.J.Kim, D.Zhang, D.C.Yang (2016) Biological synthesis of nanoparticles. Trends Biotechnol, 34, 588–599. doi: 10.1016/j.tibtech.2016.02.006

[18] K.A.Bogle, S.D.Dhole, V.N.Bhoraskar (2006) Silver nanoparticles: synthesis by UV irradiation. Nanotechnology, 17, 3204–3208. doi:10.1088/0957-4484/17/13/020

[19] S.K.Srikar, D.D.Giri, D.B.Pal, et al (2016) Green synthesis of silver nanoparticles. Green Sustain Chem, 6, 34–56. doi:10.4236/gsc.2016.61004

[20] M.A.Irshad, R.Nawaz, M.Z.Rehman, et al (2020) Photo-assisted green synthesis of nanoparticles. J PhotochemPhotobiol B, 202, 111682. doi: 10.1016/j.jphotobiol.2019.111682

[21] T.M.Abdelghany, A.M.H.Al-Rajhi, M.A.AlAbboud, et al (2018) Recent advances in green synthesis of nanoparticles. Microorganisms, 6, 36. doi:10.3390/microorganisms6020036

[22] Y.Hilal, U.Engelhardt (2007) Characterisation of white tea. J VerbrauchLebensm, 2, 414–421. doi:10.1007/s00003-007-0250-3

[23] P.K. Jain, D. Das, P. Jain (2016) Botanical authentication of medicinal plants. Indian J Tradit Knowl, 15, 215–220

[24] A.I.Vogel (1989) Vogel's textbook of practical organic chemistry. 5th ed. Longman

[25] J.Y.Song, B.S.Kim (2009) Rapid biological synthesis of silver nanoparticles. Bioprocess BiosystEng, 32, 79–84. doi:10.1007/s00449-008-0224-6

[26] M. Nasrollahzadeh, S.M. Sajadi (2015) Green synthesis of copper nanoparticles using Ginkgo biloba. J Colloid Interface Sci, 457, 141–147. doi: 10.1016/j.jcis.2015.07.004

[27] M. Rai, A.P. Ingle, S.Birla, et al (2016) Strategic role of nanoparticles in medicine. Crit Rev Microbiol, 42, 696–719. doi:10.3109/1040841X.2015.1018131

[28] K.L.Kelly, E.Coronado, L.L.Zhao, G.C.Schatz (2003) Optical properties of metal nanoparticles. J PhysChem B, 107, 668–677. doi:10.1021/jp026731y

[29] J.Coates (2000) Interpretation of infrared spectra. In: Encyclopedia of Analytical Chemistry. Wiley. doi:10.1002/9780470027318.a5606

[30] A.W.Bauer, W.M.M.Kirby, J.C.Sherris, M.Turck (1966) Antibiotic susceptibility testing by a standardized single disk method. Am J ClinPathol, 45, 493–496. doi:10.1093/ajcp/45.4_ts.493

[31] CLSI (2020) Performance standards for antimicrobial susceptibility testing. CLSI document M100

[32] S.Link, M.A.El-Sayed (1999) Size and temperature dependence of plasmon absorption of gold nanoparticles. J PhysChem B, 103, 4212–4217. doi:10.1021/jp984796o

[33] V.Amendola, M.Meneghetti (2009) Size evaluation of gold nanoparticles by UV–Vis spectroscopy. J PhysChem C, 113, 4277–4285. doi:10.1021/jp8082425

[34] G.Socrates (2001) Infrared and Raman characteristic group frequencies. Wiley

[35] B.D.Cullity, S.R.Stock (2001) Elements of X-ray diffraction. 3rd ed. Prentice Hall

[36] A.L.Patterson (1939) The Scherrer formula for X-ray particle size determination. Phys Rev, 56, 978–982. doi:10.1103/PhysRev.56.978

[37] R.J.Hunter (1981) Zeta potential in colloid science. Academic Press

[38] S.Bhattacharjee (2016) DLS and zeta potential – What they are and what they are not. J Control Release, 235, 337–351. doi:10.1016/j.jconrel.2016.06.017

[39] G.Ren, D.Hu, E.W.C.Cheng, et al (2009) Characterisation of copper oxide nanoparticles antimicrobial study. Int J Antimicrob Agents, 33, 587–590. doi:10.1016/j.ijantimicag.2008.12.004

[40] M.Rai, A.Yadav, A.Gade (2009) Silver nanoparticles as a new generation of antimicrobials. Biotechnol Adv, 27, 76–83. doi:10.1016/j.biotechadv.2008.09.002

IZVOD

ZELENA SINTEZA CuNP KORIŠĆENJEM *CAMELLIA SINENSIS* I *OCIMUM SANCTUM* POD UV SVETLOŠĆU

Razvoj ekološki prihvatljivih načina za sintezu metalnih nanočestica je važan cilj u savremenim istraživanjima nanomaterijala, posebno radi minimiziranja oslanjanja na toksične hemijske redukcione i stabilizatore. U ovoj studiji, nanočestice bakra (CuNP) su sintetizovane korišćenjem vodenih ekstrakata Camellia sinensis (zeleni čaj) i Ocimum sanctum (tulsi), koji su istovremeno funkcionisali kao redukcioni i zatvarajući agensi. Sistematski su ispitana dva načina sinteze: konvencionalni fitogeni proces redukcije i ultraljubičasti (UV-A, 365 nm) fotoredukcijski pristup. U konvencionalnoj metodi, postepena redukcija Cu^{2+} jona tokom 3 sata dala je pretežno sferne CuNP sa veličinama čestica u opsegu od 20–50 nm i zeta potencijalom od -29,5 mV, što ukazuje na umerenu koloidnu stabilnost. Nasuprot tome, UV-pomognuta sinteza značajno je ubrzala formiranje nanočestica, završavajući reakciju u roku od 15–20 minuta i proizvodeći manje čestice (8–25 nm) sa poboljšanom stabilnošću (zeta potencijal između -30 i -38 mV). UV-vidljiva spektroskopija je otkrila jasne površinske plazmonske rezonantne trake za oba uzorka, pri čemu UV-pomognute CuNP pokazuju oštriji i blago plavo pomeren vrh, što je u skladu sa smanjenom veličinom čestica i užom raspodelom veličine. Furijeova transformaciona infracrvena spektroskopija potvrdila je učešće polifenolnih i fenolnih sastojaka, uključujući delove tipa katehina i eugenola, u redukciji i stabilizaciji CuNP. Analiza rendgenske difrakcije potvrdila je formiranje kristalnog kubnog bakra centriranog na površini sa manjim doprinosima Cu_2O, dok je transmisiona elektronska mikroskopija potvrdila poboljšanu uniformnost UV-pomognutih nanočestica. Antibakterijska aktivnost sintetisanih CuNP je procenjena u odnosu na Escherichia coli i Staphylococcus aureus, otkrivajući efikasnu inhibiciju rasta za oba bakterijska soja. UV-pomognute CuNP pokazale su neznatno veću antibakterijsku efikasnost, što se pripisuje njihovoj manjoj veličini i poboljšanoj površinskoj stabilizaciji. Generalno, ova studija pokazuje da UV-pomognuta fitogena sinteza nudi brz i reproduktivn put do stabilnih nanočestica bakra, uz očuvanje prednosti zelene hemije. Rezultati ističu potencijal kombinovanja reduktanata biljnog porekla sa fotohemijskom aktivacijom kako bi se postigla kontrolisana sinteza nanočestica za antimikrobne i srodne primene.

Ključne reči: *Zelena sinteza, nanočestice bakra, UV-pomognuta fotoredukcija, Camellia sinensis, Ocimum sanctum, antimikrobna aktivnost, održiva nanotehnologija*

naučni rad
rad primljen 16.03.2026
rad prihvacen 2.04.2026.

Naveen Pathivada: https://orcid.org/0009-0003-1664-1988
Gopi Mamidi: https://orcid.org/0009-0009-1248-7745

Aman Charla Indira Priyadarsini: https://orcid.org/0009-0005-3118-2024
Gunduluru Swathi: https://orcid.org/0009-0005-9008-9532